Uses and Limitations of Micro-Synchrophasor Measurements in Distribution Grid Management

Kyle Brady

Electrical Engineering and Computer Sciences
University of California at Berkeley

Technical Report No. UCB/EECS-2016-80
http://www.eecs.berkeley.edu/Pubs/TechRpts/2016/EECS-2016-80.html

May 13, 2016

Uses and Limitations of Micro-Synchrophasor Measurements in Distribution Grid Management

by Kyle Brady

Research Project

Submitted to the Department of Electrical Engineering and Computer Sciences, University of California at Berkeley, in partial satisfaction of the requirements for the degree of **Master of Science, Plan II**.

Approval for the Report and Comprehensive Examination:

Committee:

Alexandra von Meier
Research Advisor

Date

* * * * * *

Duncan Callaway
Second Reader

Date

Acknowledgments

I would like to take this opportunity to thank Sascha von Meier for being an excellent research advisor, mentor, and rock climbing partner. I've truly appreciated all your ideas and encouragement throughout my time at Berkeley. I would also like to thank the students who have either been members of or worked with my research group for the past two years: Dan Arnold, Michael Sankur, Roel Dobbe, Oscar Sondermeijer, Omid Ardakanian, and Christine Abelyan. Thanks also to Ioannis Konstantakopolous for his tireless efforts to create a workable means of solving our line impedance estimation problem. Another thanks goes out to Emma Stewart, Ciaran Roberts, Emre Kara, and Anna Liao at the Lawrence Berkeley Lab, and to everyone at the Amp Lab for their excellent work in developing and maintaining the BTrDB plotter. Finally, I would like to thank Liz Kraushar for all of her support in everything I've done.

Abstract

This report is a partial summary of a research project that explores the use of synchrophasor measurements at the distribution level of the electric grid. The project, which is sponsored by ARPA-E, is now concluding its third year of work. During that time, a huge amount of analytical effort has been undertaken by a number of researchers and students. That effort has been aimed at everything from basic science applications to the advancement of an operational and commercial case for synchrophasors in distribution systems. A sampling of these efforts are included in this report, which is intended to double as a collection of updates that can be provided to individual research partners. Therefore, the chapters into which it is divided are modular and can be read in any order. The topics covered include: the initial performance validation of the Phasor Measurement Units (PMUs) used in the project, along with their comparison to the present state of the art in voltage measurement; a methodology for estimating line impedance from PMU measurements and a description of a case in which it was successfully implemented; the limitations of that methodology due to the specifics of another PMU deployment and an analysis of that failure case; and an ongoing examination of voltage volatility and its potential application to customer-side PV discovery.

Introduction

The following report is a summary of several studies undertaken for the ARPA-E project "Micro-Synchrophasors for Distribution Systems." The research sponsored by this project explored the possibilities for introducing synchrophasor data from Phasor Measurement Units (PMUs) to the standard suite of tools used in analysis and operations at the distribution level of the electric grid.

PMUs, which enable extremely precise measurement of voltages and currents, are a mature technology widely used throughout high-voltage transmission applications. They have not yet been utilized in lower-voltage, distribution-level operations, though, in part because electric failures and power outages at the distribution level are much less costly. Hence, the business case for advanced sensing is less clear. Our research group hopes to demonstrate the potential of synchrophasor data at these lower voltage levels through the deployment of a network of PMUs on distribution feeders throughout the country and analysis of the data returned.

We have installed μPMU-brand PMUs, developed by Power Standards Laboratory in Alameda, on a number of distribution feeders managed by utility partners and other cooperating agencies. These μPMUs are capable of sampling both voltages and currents 512 times per cycle on three phases simultaneously, for a total of six data streams per μPMU. After the data is processed on the device, it is reported 120 times per second as a set of voltage and current phasors with an accuracy of $.002^\circ$ in angle and 2PPM magnitude resolution.

Time series phasor magnitude and angle data is then maintained in the Berkeley Tree Database (BTrDB), a data storage system designed by Michael Andersen and David Culler of Berkeley's Computer Science Department. The data can be accessed through a convenient online plotter, which also allows for five-minute increments of .csv formatted data to be pulled onto a local machine. More specialized time intervals can be pulled as needed using Python scripts, which are also used to implement a distillate framework in which voltage and current phasors are used as inputs to calculations that produce other data in near real time. With this structure, network characteristics of interest such as frequency, phase angle differences between points, and real/reactive power can be used in analysis as easily as can raw voltage/current data streams.

Our research group has performed a large amount of analysis on the available data, which amounts to nearly a year's worth of measurements for some of the longer-running μPMUs. Due to the specifics of individual μPMU deployments, different types of analysis were conducted at different locations. As such, this report will be divided into modular chapters, with each chapter covering a single operating utility or research partner. There may be some repetition of basic information about μPMU operation or data between chapters, as each chapter is also meant to stand alone as a project update that can be provided to the relevant partner. In particular, a description of the mathematical procedure for using μPMU measurements to estimate the impedance of a three-phase line (the subsections titled "Methodology") will be very similar in both the *Partner 2* and *Partner 3* chapters.

A few other notes on layout:

- Citations will be included as footnotes, rather than endnotes.
- Figure, table, and footnote numbering will be restarted at the beginning of each chapter, and so any figure numbers should be understood to refer to the figures within the chapter in which they were mentioned.
- The names of partnering utilities and distribution feeder operators have been redacted and replaced with "Partner numbers" where necessary due to customer privacy concerns.

Chapter 1: Validation of μPMU Performance at NEETRAC

Our research team sent five μPMUs to Georgia Tech for performance validation by comparison with the existing instrumentation in their NEETRAC test bed. The test bed is made up of five interconnected buses with a controllable voltage magnitudes and phasor angles. Two of those buses, numbered 1 and 5, are electrically connected and the other three (Buses 2, 3 and 4) are connected through three-phase high-inductance lines as shown in Figure 1.

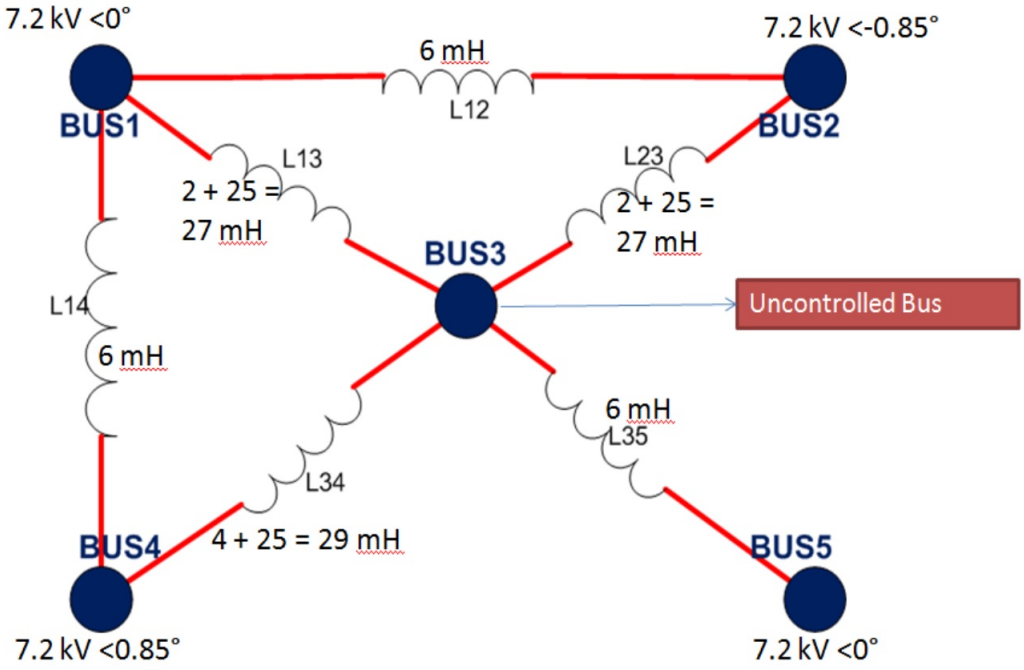

Figure 1: The electrical connections at the NEETRAC testbed.

The μPMUs were connected alongside NEETRAC's own National Instruments-built PMUs at each of the five buses shown above and used to gather two hours of data: August 21, 2015, 17:00 and 18:00 UTC. Unfortunately, difficulties in transferring that data resulted in the loss of all measurements from Bus 1. Because the data collected at Bus 1 and Bus 5 were redundant, though, this did not pose any problems for our team's efforts.

To validate the data collected from the μPMUs at Bus 2 through Bus 5 against the measurements of the NI PMUs, NEETRAC used the following experimental procedure (All times listed below are given as UTC):

- 17:49.51: Began slowly raising the test bed voltage magnitude on all three phases.
- 17:51:30: Test bed voltage magnitude reaches its maximum value of approximately 7.2 kV.
- 17:51:59: Phase shifters begin changing the voltage phase of Buses 2 and 4 relative to Bus 5 in the order Phase A-Phase B-Phase C. Each phase shift is separated by several seconds.
- 17:52:10: Phase values at Buses 2 and 4 reach their maximum difference of 0.85 degrees.
- 17:53:46: Phase values are stepped back down to near zero over several seconds, again with a slight delay between phases.
- 17:54:11: Test bed voltage is stepped back down to near zero over approximately a minute.

A sample of the resulting measurements is shown in Figures 2 and 3. As can be seen, there is good agreement between the μPMU observations and the NEETRAC PMU measurements in both voltage magnitude and phase angle. Some calibration is necessary, though, to take into account the differences in PMU reporting:

- The NEETRAC PMU:μPMU voltage and current magnitude ratios were 60:1 and 300:1, respectively.
- The time stamps between the NEETRAC PMUs and μPMUs were offset by 4 hours and 1 minute (e.g. 13:00 by the NEETRAC PMU clock would be 17:01 by the μPMU clock). This can be ignored in the figures below, though, as the hours of the timestamps are aligned for comparison in the display.
- μPMU data will occasionally change the sign of its angular representation, e.g. 120 degrees will spontaneously become -240 degrees. Though this can be confusing graphically, in absolute terms the μPMU measurements are consistent with those of the NEETRAC PMUs throughout the testing period.

Accounting for the shift in timestamps, it is clear that both the μPMUs and NEETRAC's PMUs are measuring the same test bed voltage. The agreement in angular difference is also very close, and holds for both buses 2 and 4, as expected. Based on these observations, we have high confidence that the μPMU measurements at buses 2 through 5 are generally accurate.

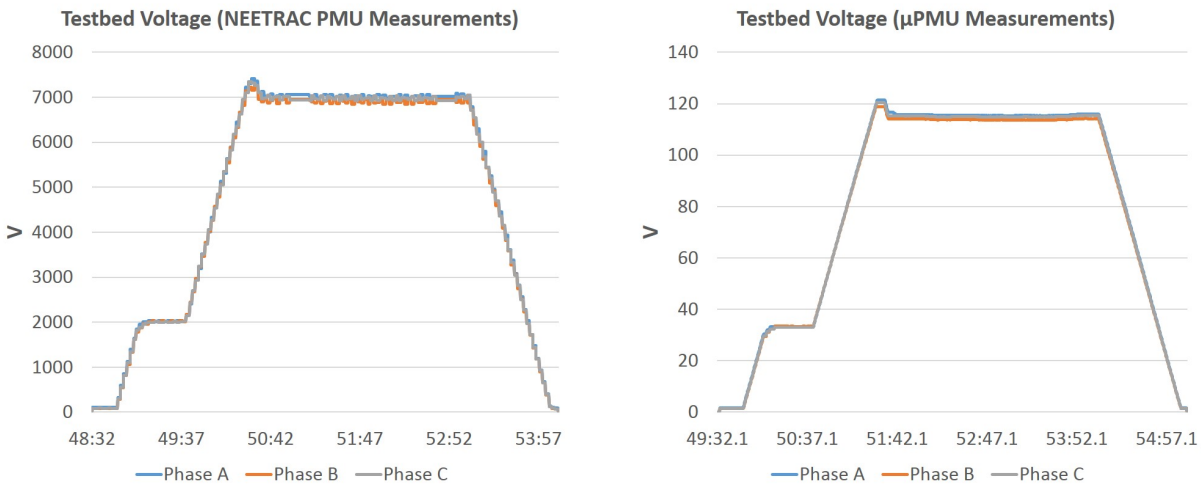

Figure 2: Testbed voltage measurements, NEETRAC NI PMU vs μPMU.

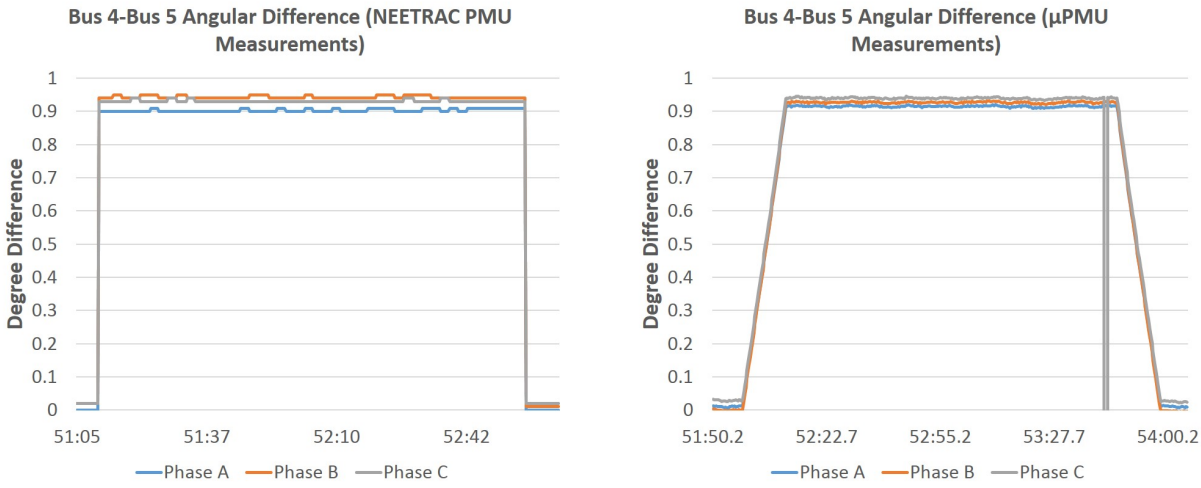

Figure 3: The angular difference at bus 4 relative to bus 5. The dip in angular difference on Phase C represents a point at which the μPMU's angular representation shifts by 360 degrees and then quickly returns.

Two things are worth noting in Figures 2 and 3. The first is that the μPMU measurements are of a higher precision than those of the PMUs in use at NEETRAC. This is not a commentary on the National Instruments PMUs themselves, as user-defined settings play a significant role in the nature of the data that is captured and reported. Rather, this is an observation that the data being collected in BTrDB is of a precision beyond what NEETRAC has found sufficient for their research purposes to date.

The second interesting point revealed by the measurement comparison is that there is disagreement as to the ordering of the phase angle differences in Figure 3. While the NEETRAC PMUs generally show the angle differences as slightly larger on Phase B than on Phase C, the μPMUs report the opposite. The reason for this is still an open question. Technicians at NEETRAC have confirmed that all connections for both μPMUs and NI PMUs were made correctly, which is corroborated by the agreement between the two sets of PMUs on the ordering of voltage magnitudes in Figure 2. It is possible that the disagreement is due to the difference in measurement precision between the two sets of PMUs. In any event, any discrepancies are small enough that this can be considered a successful validation of μPMU capabilities.

Chapter 2: Line Impedance Estimation at Partner 2

As an inital step towards model validation applications, our research team has begun to explore the network parameters that can be estimated from μPMU data. Specifically, we have begun by attempting to determine the impedances of lines and other equipment in the area of our μPMU deployments.

Six μPMUs are presently deployed in and are reporting data from feeders owned by Partner 2. Among them are two μPMUs connected on a feeder between the substation and a 7.5MW PV site, as shown in Figure 1. In combination, these two μPMUs present us with a simple base case: data reporting from either side of a three-phase connecting line. We used the data from these μPMUs to estimate the impedance of that line, which connects the substation and the point of common coupling (PCC) of the PV site.

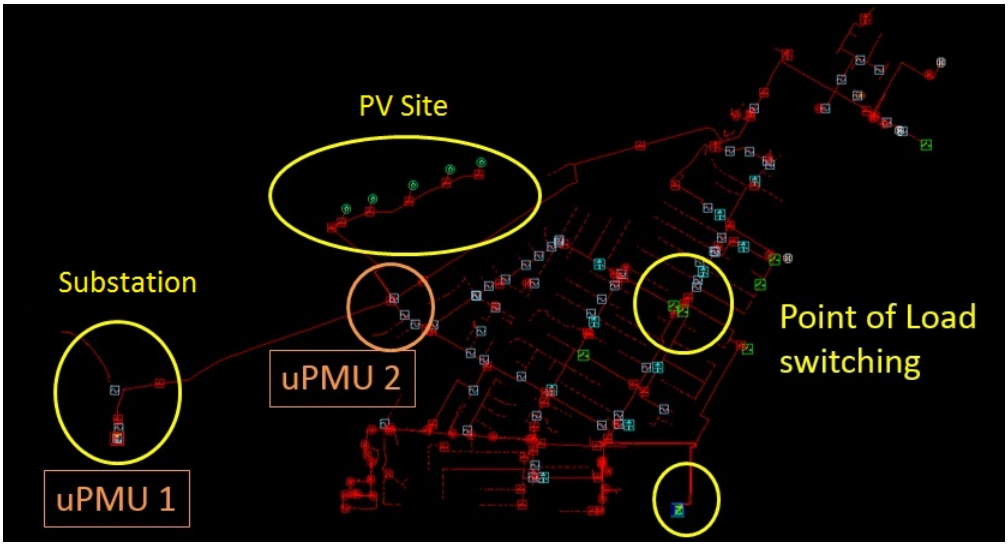

Figure 1: μPMU deployment at Partner 2's feeder.

Methodology

In this section, we describe the mathematics of our impedance estimation method. We designate the two μPMUs on either side of the three-phase line connecting the substation and the PCC as α and β, respectively. Each μPMU delivers 120 samples per second, and each sample gives us a 3x1 V_{ABC} vector and a 3x1 I_{ABC} vector, where A, B, and C denote phases.

For each sample, the relationships below follow from Ohm's Law:

$$\begin{aligned}\vec{V}_{\alpha A} - \vec{V}_{\beta A} &= \vec{Z}_{AA}\vec{I}_A + \vec{Z}_{AB}\vec{I}_B + \vec{Z}_{AC}\vec{I}_C \\ \vec{V}_{\alpha B} - \vec{V}_{\beta B} &= \vec{Z}_{\epsilon AB}\vec{I}_A + \vec{Z}_{BB}\vec{I}_B + \vec{Z}_{BC}\vec{I}_C \\ \vec{V}_{\alpha C} - \vec{V}_{\beta C} &= \vec{Z}_{AC}\vec{I}_A + \vec{Z}_{BC}\vec{I}_B + \vec{Z}_{CC}\vec{I}_C\end{aligned} \tag{1}$$

In reality, the β μPMU (labeled "uPMU 2" in Figure 1) is located slightly north of the PCC, on the line connecting the PV site. It is close enough, though, that the voltage drop between the μPMU and the PCC is negligible and we can approximate the μPMU-measured voltage as the PCC voltage V_β. The current measurement will be very different from that of the connecting line, however, and so we will need to use μPMU α to measure the current on our line of interest. Therefore, $\vec{I}_A = \vec{I}_{\alpha A}$, $\vec{I}_B = \vec{I}_{\alpha B}$, and $\vec{I}_C = \vec{I}_{\alpha C}$.

To estimate the six unique elements of the impedance matrix, $\vec{Z}_{AA}$ through $\vec{Z}_{CC}$, we break equations (1) into their complex parts and use the real component to relate impedances and μPMU measurements:

$$\begin{aligned}&\Re(V_{\alpha A}) - \Re(V_{\beta A}) = \\ &\Re(I_A)\Re(Z_{AA}) - \Im(I_A)\Im(Z_{AA}) - \Im(I_B)\Im(Z_{AB}) + \Re(I_B)\Re(Z_{AB}) - \Im(I_C)\Im(Z_{AC}) + \Re(I_C)\Re(Z_{AC}) \\ \\ &\Re(V_{\alpha B}) - \Re(V_{\beta B}) = \\ &\Re(I_A)\Re(Z_{AB}) - \Im(I_A)\Im(Z_{AB}) - \Im(I_B)\Im(Z_{BB}) + \Re(I_B)\Re(Z_{BB}) - \Im(I_C)\Im(Z_{BC}) + \Re(I_C)\Re(Z_{BC}) \\ \\ &\Re(V_{\alpha C}) - \Re(V_{\beta C}) = \\ &\Re(I_A)\Re(Z_{AC}) - \Im(I_A)\Im(Z_{AC}) - \Im(I_B)\Im(Z_{BC}) + \Re(I_B)\Re(Z_{BC}) - \Im(I_C)\Im(Z_{CC}) + \Re(I_C)\Re(Z_{CC})\end{aligned} \tag{2}$$

Though we have dropped the vector notation in equations (2) and will omit it moving forward, all V, I, Z quantities should be understood to be complex-valued.

Equations (2) can be solved for the real and imaginary parts of the six unique impedance elements with a number of methods including least squares, gradient descent, and coordinate descent. We did not find any significant differences in accuracy between these three methods. As such, we will not present all three as separate cases, instead focusing only on ordinary least squares (OLS).

Recasting equations (2) into an OLS matrix form:

$$\begin{bmatrix} \Re(V_{\alpha A}) - \Re(V_{\beta A}) \\ \Re(V_{\alpha B}) - \Re(V_{\beta B}) \\ \Re(V_{\alpha C}) - \Re(V_{\beta C}) \end{bmatrix} =$$

$$\begin{bmatrix} \Re(I_A) & -\Im(I_A) & 0 & 0 & 0 & 0 & \Re(I_B) & -\Im(I_B) & \Re(I_C) & -\Im(I_C) & 0 & 0 \\ 0 & 0 & \Re(I_B) & -\Im(I_B) & 0 & 0 & \Re(I_A) & -\Im(I_A) & 0 & 0 & \Re(I_C) & -\Im(I_C) \\ 0 & 0 & 0 & 0 & \Re(I_C) & -\Im(I_C) & 0 & 0 & \Re(I_A) & -\Im(I_A) & \Re(I_B) & -\Im(I_B) \end{bmatrix} *$$

$$\begin{bmatrix} \Re(Z_{AA}) \\ \Im(Z_{AA}) \\ \Re(Z_{BB}) \\ \Im(Z_{BB}) \\ \Re(Z_{CC}) \\ \Im(Z_{CC}) \\ \Re(Z_{AB}) \\ \Im(Z_{AB}) \\ \Re(Z_{AC}) \\ \Im(Z_{AC}) \\ \Re(Z_{BC}) \\ \Im(Z_{BC}) \end{bmatrix} \quad (3)$$

The three equations generated by each new sample can be added to the voltage vector and to the matrix of currents until it is of full rank, at which point the impedance can be estimated with OLS.

Results

We carried out the OLS impedance estimation methodology on a 25-second block of μPMU data, arbitrarily chosen to begin at noon on October 21, 2015. Feeder models from Partner 2 provided our group with a "ground truth" value against which to compare our results. Written as a

vector, the modeled impedance of the cable is given as $\begin{bmatrix} \Re(Z_{AA}) \\ \Re(Z_{BB}) \\ \Re(Z_{CC}) \\ \Re(Z_{AB}) \\ \Re(Z_{AC}) \\ \Re(Z_{BC}) \end{bmatrix} = \begin{bmatrix} 0.523 + 1.135j \\ 0.523 + 1.135j \\ 0.523 + 1.135j \\ 0.146 + 0.387j \\ 0.146 + 0.387j \\ 0.146 + 0.387j \end{bmatrix}$, while the OLS method returns $\begin{bmatrix} \Re(Z_{AA}) \\ \Re(Z_{BB}) \\ \Re(Z_{CC}) \\ \Re(Z_{AB}) \\ \Re(Z_{AC}) \\ \Re(Z_{BC}) \end{bmatrix} = \begin{bmatrix} 0.5 + 1.29j \\ 0.59 + 1.24j \\ 0.45 + 1.08j \\ 0.12 + 0.37j \\ 0.21 + 0.18j \\ 0.1 + 0.29j \end{bmatrix}$.

This gives us a total vector error of 14.4%, as defined in terms of vector 2-norms.

This is reasonably good agreement, with several well-understood sources of error that could account for the discrepancy. First, the values from Partner 2's model doubtless have some error; it is very unlikely that the self and mutual impedance values of the line are completely uniform, as stated. It is possible that the OLS-estimated values are closer to the true impedance of the line than is our ground truth. We also must consider the error introduced by the voltage drop across the small line segment connecting the PCC to the true location of μPMU #2. Without a more rigorous physical examination to determine the precise properties of the line, it is impossible to know exactly how accurate are the results of the OLS estimation. However, given the reasonable agreement between the OLS results and the modeled impedance values, we believe we have developed a serviceable method of impedance estimation for use on distribution lines.

It is worth mentioning that this same method failed when applied to much shorter cables on a feeder owned by another research partner. This was most likely due to an insufficiently high voltage drop across the cable, which was then lost in the noise introduced by instrumentation transformers at the μPMU inputs. Future work on this topic could involve searching for the minimum data excitation vs. noise threshold past which it is no longer possible to use OLS to estimate line impedance.

Chapter 3: Difficulties with Line Impedance Estimation at Partner 3

A number of μPMUs have been deployed on a feeder at Partner 3. Among them are two matched sets of μPMUs on either side of two underground cables, Cable X and Cable Y, which are connected on different branches of the feeder. We used the data from these μPMUs in an effort to establish that, with sufficient μPMU measurements from either side of a cable, we would be able to determine the impedance of the cable itself.

Though we developed a straightforward model for which impedance could be accurately estimated on sets of simulated data, we were unsuccessful implementing it in the field. We found that the measurement error introduced by instrumentation transformers created noise that interfered with our ability to solve the set of equations relating our μPMU data to the desired impedance values. This noise was especially significant at Partner 3, as the cables that we used as test cases were short and had low resistance that did not cause a significant voltage drop. A similar test of our method on a longer cable at another utility partner was more successful.

Methodology

In this section, we describe the mathematics of our impedance estimation method. We designate the two μPMUs on either side of the three-phase line as α and β. Each μPMU delivers 120 samples per second, and each sample gives us a 3x1 V_{ABC} vector and a 3x1 I_{ABC} vector, where A, B, and C denote phases. For each sample, the relationships below follow from Ohm's Law:

$$\begin{aligned} \vec{V}_{\alpha A} - \vec{V}_{\beta A} &= \vec{Z}_{AA}\vec{I}_A + \vec{Z}_{AB}\vec{I}_B + \vec{Z}_{AC}\vec{I}_C \\ \vec{V}_{\alpha B} - \vec{V}_{\beta B} &= \vec{Z}_{\epsilon AB}\vec{I}_A + \vec{Z}_{BB}\vec{I}_B + \vec{Z}_{BC}\vec{I}_C \\ \vec{V}_{\alpha C} - \vec{V}_{\beta C} &= \vec{Z}_{AC}\vec{I}_A + \vec{Z}_{BC}\vec{I}_B + \vec{Z}_{CC}\vec{I}_C \end{aligned} \tag{1}$$

Note that the equations (1) involve the approximation $I_\alpha = I_\beta = I$. In reality, the currents measured at either side of the cable are slightly different. But, the effect is very small and trying to take it into account would introduce massive mathematical complexity into the modeling effort.

To estimate the six unique elements of the impedance matrix, $\vec{Z}_{AA}$ through $\vec{Z}_{CC}$, we break

equations (1) into their complex parts and use the following real equations:

$$\Re(V_{\alpha A}) - \Re(V_{\beta A}) =$$
$$\Re(I_A)\Re(Z_{AA}) - \Im(I_A)\Im(Z_{AA}) - \Im(I_B)\Im(Z_{AB}) + \Re(I_B)\Re(Z_{AB}) - \Im(I_C)\Im(Z_{AC}) + \Re(I_C)\Re(Z_{AC})$$

$$\Re(V_{\alpha B}) - \Re(V_{\beta B}) =$$
$$\Re(I_A)\Re(Z_{AB}) - \Im(I_A)\Im(Z_{AB}) - \Im(I_B)\Im(Z_{BB}) + \Re(I_B)\Re(Z_{BB}) - \Im(I_C)\Im(Z_{BC}) + \Re(I_C)\Re(Z_{BC})$$

$$\Re(V_{\alpha C}) - \Re(V_{\beta C}) =$$
$$\Re(I_A)\Re(Z_{AC}) - \Im(I_A)\Im(Z_{AC}) - \Im(I_B)\Im(Z_{BC}) + \Re(I_B)\Re(Z_{BC}) - \Im(I_C)\Im(Z_{CC}) + \Re(I_C)\Re(Z_{CC}) \tag{2}$$

Though we have dropped the vector notation in equations (2) and will omit it moving forward, all quantities should be understood to be complex-valued.

Equations (2) can be solved for the real and imaginary parts of the six unique impedance elements with either ordinary least squares (OLS) or one of a number of other options. In addition to OLS, we attempted three more advanced methods at Partner 3:

Constrained Least Squares: This method uses the standard equation for solving a linear least squares problem of the form $Ax = b$, with the solution bounded to return positive real portions of the impedance. In practice, the bounds were unnecessary for our synthetic data in the cases where we obtained a successful estimation, in which cases the method reduces to OLS.

Coordinate Descent: Coordinate descent is an iterative technique for minimizing a function. It solves the $Ax = b$ equation by moving through the x vector element-by-element, starting from an initial guess of the value of x. Every iteration updates a single element of the x vector using the formula $x_i = A_i^*(b - A_{-i}x_{-i})/(A_i^*A_i)$.

Gradient Descent: For future applications, we expect gradient descent to be the most effective method for dealing with field data. It avoids the problems associated with both least squares (which may require more widely varying currents and voltages than are available on Cable X or Y in order to be a well-conditioned matrix) and with coordinate descent (which is not guaranteed to converge, even for convex functions). Gradient descent is essentially no different from coordinate descent,

except that it simultaneously updates all of the elements in its x vector with every iteration. During the iteration, x is updated according to the formula $x_n = x_{n-1} - 2A^*(Ax_{n-1} - b)\gamma$, where γ is an arbitrary step size.

We did not find any significant differences in accuracy between these three methods; all three were very successful when used on simulated data with minimal errors, but failed when applied to Partner 3's underground cables. As such, we will not present the results of all four methods as separate cases, instead focusing only on ordinary least squares (OLS).

We recast equations (2) into a matrix form for use in OLS:

$$\begin{bmatrix} \Re(V_{\alpha A}) - \Re(V_{\beta A}) \\ \Re(V_{\alpha B}) - \Re(V_{\beta B}) \\ \Re(V_{\alpha C}) - \Re(V_{\beta C}) \end{bmatrix} =$$

$$\begin{bmatrix} \Re(I_A) & -\Im(I_A) & 0 & 0 & 0 & 0 & \Re(I_B) & -\Im(I_B) & \Re(I_C) & -\Im(I_C) & 0 & 0 \\ 0 & 0 & \Re(I_B) & -\Im(I_B) & 0 & 0 & \Re(I_A) & -\Im(I_A) & 0 & 0 & \Re(I_C) & -\Im(I_C) \\ 0 & 0 & 0 & 0 & \Re(I_C) & -\Im(I_C) & 0 & 0 & \Re(I_A) & -\Im(I_A) & \Re(I_B) & -\Im(I_B) \end{bmatrix} *$$

$$\begin{bmatrix} \Re(Z_{AA}) \\ \Im(Z_{AA}) \\ \Re(Z_{BB}) \\ \Im(Z_{BB}) \\ \Re(Z_{CC}) \\ \Im(Z_{CC}) \\ \Re(Z_{AB}) \\ \Im(Z_{AB}) \\ \Re(Z_{AC}) \\ \Im(Z_{AC}) \\ \Re(Z_{BC}) \\ \Im(Z_{BC}) \end{bmatrix} \quad (3)$$

The three equations generated by each new sample can be added to the voltage vector and to the matrix of currents until it is of full rank, at which point the impedance can be estimated with OLS.

Synthetic Data Results

Using MATLAB, we generated a set of synthetic data to serve as a proof of the impedance estimation method. This began with the creation of 3-phase currents by generating sets of three I vectors. The distribution of the I vector angles was completely random, while the magnitudes were constrained to lie between 25 and 50. These magnitude constraints were arbitrarily chosen to keep our simulation relatively realistic, though mathematically speaking the actual upper and lower magnitude bounds have no effect on the method's success or failure.

We then had to generate a three-phase voltage difference vector $\Delta\vec{V}$ that represented $\vec{V}_\alpha - \vec{V}_\beta$, the voltage difference between the α and β ends of the line. For this, we multiplied each of our synthetic, 3-phase current samples by a "ground truth" matrix of self and mutual impedance values taken from a Partner 3 feeder model. This guaranteed that our synthetic voltages and currents satisfied Ohm's Law for our assumed values of cable impedance. Each (I,V) pair generated using this technique represented what would be one μPMU sample in the total absence of measurement error of any type. As would be expected when using this error-free data, the elements of the impedance matrix could be estimated exactly with OLS using only the minimum number of samples necessary to create an invertible matrix.

We then added simulated measurement error terms to our synthetic $\Delta\vec{V}$ and $\vec{I}$ vectors. The errors were generated with random angles and Gaussian-distributed magnitudes of zero mean. We altered the size of the standard deviation of the error distribution σ_E and noted the accuracy of the OLS method at each step, as seen in Table 1. The percentage values given in the table refer to the accuracy of the impedance estimation, given by 1 less the Total Vector Error in our estimation.

	$\sigma_E = 10^{-6}$	$\sigma_E = 10^{-4}$	$\sigma_E = 10^{-2}$
10 Samples	99.216%	98.363%	13.749%
10^3 Samples	99.965%	99.065%	75.27%
10^4 Samples	99.976%	99.692%	79.38%

Table 1: OLS accuracy given σ_E and number of samples used in the OLS calculation.

As we can see, the OLS method should be more than capable of handling errors of the size ex-

pected from the μPMUs. The method is disrupted at Partner 3, though, by further error introduced by instrumentation transformers.

Transformer Measurement Error on Cables X and Y

We have yet to use field measurement data to successfully obtain an estimate of the impedance at Cable X or Cable Y that is even physically possible. Not only has OLS failed, but coordinate and gradient descent methods have as well. The most probable reason for this, as has been mentioned in previous sections, is the error introduced by the instrumentation transformers that bring line voltage down to a level at which it can be measured by a μPMU.

From the transformer's manufacturer specifications, we are given maximum possible multiplicative measurement errors of $0.003\angle 0.2^\circ$ in all voltages and $0.012\angle 1^\circ$ in all currents. These errors would primarily be due to mismatch in the transformer windings or other manufacturing defects that are constant in time. The primary hindrance to the accuracy of the OLS method, though, is time-varying error.

While it is difficult to determine to what extent transformer measurement error changes with time, one aspect of our μPMU deployment at Partner 3 can give us some idea of the order of magnitude: a second μPMU is installed on a bus to which Cable Y is connected. While this second μPMU measures a different current than does the μPMU on Cable Y itself, it is measuring a point with near-identical voltage. We would expect the two μPMUs' voltage measurements to be offset due to differences in the individual measurement errors of each transformer, but we can observe the difference between the two voltages over time as an indicator of the constancy of those measurement errors.

As can be seen in Figure 1, a representative time period, voltage magnitude measurements can range over 0.03% and $.018^\circ$ in very short time periods. An OLS estimation that makes use of even a few seconds' worth of data can see fairly wide time variance in transformer error. Compounding these fluctuations is the independent voltage error from the transformer on the opposite side of the cable, as well as the errors in current measurements generated by both transformers.

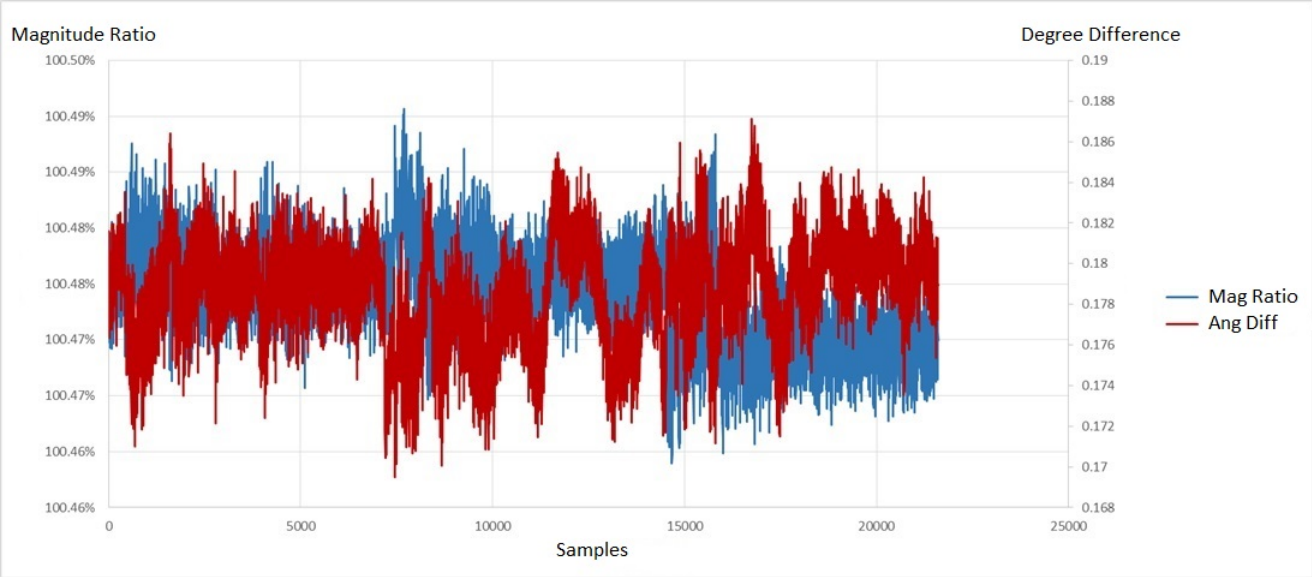

Figure 1: Time variance of measurement error over a representative interval.

Insufficiency of Current Excitation

In addition to the possible data issues caused by the time-variance of PT and CT measurement error discussed above, there are questions about the sufficiency of excitation in our current data. If the current flowing through Cable X, for example, does not change over the 5-minute data sets that we examine, our methods will not be able to estimate line impedance in the presence of noise, regardless of how well that noise is suppressed or accounted for. In addition, the current must change differently on different phases in order for the effects of self and mutual impedance to be distinguished.

The excitation problem can best be visualized as a distribution of the per-sample change of the difference between currents on separate phases. This is displayed in Figures 2 and 3, which were generated from a representative 5-minute set of Cable X current measurements. To create the figure, we began by taking the magnitude difference in currents flowing in phases A and B ($I_{A0} - I_{B0}$) for a single sample. That difference was then compared with the same difference for the succeeding sample ($I_{A1} - I_{B1}$), and binned according to the quantity $(I_{A1} - I_{B1}) - (I_{A0} - I_{B0})$. This distribution of the difference in time of the difference between two phases gives us some idea of the cross-phase variability of currents, the component of the data necessary for separating and accounting for the effects of self and mutual impedances.

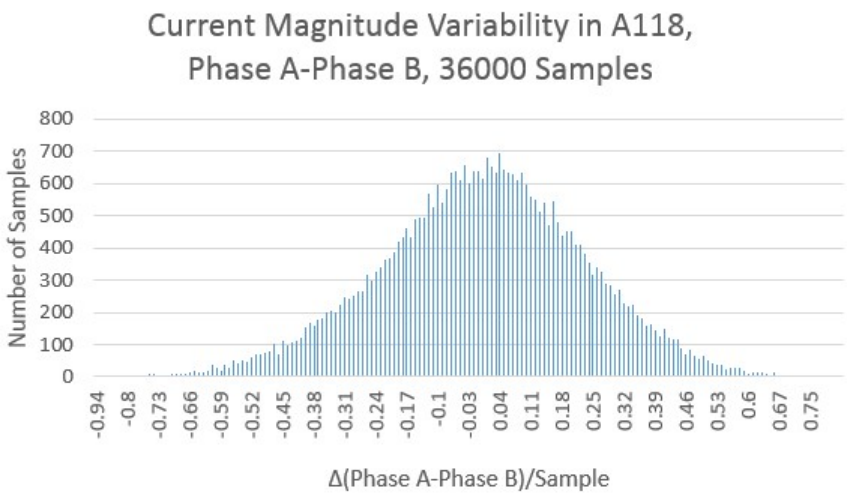

Figure 2: Current vector magnitude variability

A similar chart for phase difference:

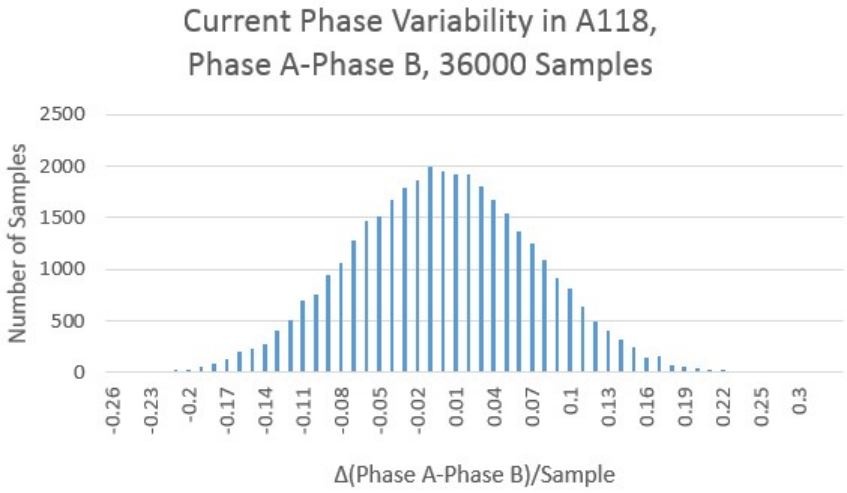

Figure 3: Current phase angle variability

We believe that these sets of data lie below a minimum excitation threshold past which the current is too small for any of our methods to return a reasonable solution. Experimentation with the bounds on the variability of current used to generate our synthetic data indicates that such a point does indeed exist, even when PT and CT error are perfectly constant. Future analysis will involve establishing precisely where that point lies, which will allow us to quickly determine which data

sets are suitable candidates for impedance analysis.

Conclusion

At Partner 3, the measurement errors are significant enough relative to our signal of interest that our OLS method can not be used. At other locations, though, it has had some success in returning an estimate that roughly agrees with modeled values. It is possible that, with some refinement, the impedance estimation could be made to work at Partner 3 as well. More advanced techniques for handling transformer error in the input to μPMUs, which have been explored at the transmission level,[1] could be incorporated into the method. We could also experiment with the averages of large numbers of OLS solutions carried out on very small time periods (on the order of several cycles) that would be less prone to measurement error fluctuation. On recommendation from our project's sponsors, though, we are no longer pursuing impedance estimation methods at Partner 3 for the time being.

[1]Pal, A., Chatterjee, P., Thorp, J. S., & Centeno, V. A. (2016). Online Calibration of Voltage Transformers Using Synchrophasor Measurements. *IEEE Transactions on Power Delivery, 31*(1), 370-380. doi:10.1109/tpwrd.2015.2494058

Ongoing Work: Voltage Volatility Studies at Partner 4

Our research group's μPMU deployment at Partner 4 encompasses five devices deployed on two adjacent feeders served by a single substation. Four of the devices are spread throughout the northern, "Alpha" feeder, while the fifth monitors a location near the substation on the southern, "Beta" feeder. Due to customer privacy concerns, these μPMUs are limited to measuring only voltages, without reporting any current data.

Though we do not have comprehensive load data for either feeder, it is known that some of the customers on the Alpha circuit have connected PV generators. This makes Partner 4 an ideal candidate for testing the suitability of μPMU measurements for use in load identification applications. If synchrophasor data can be used to uncover and characterize PV generation behind the meter, this will be a valuable use case for distribution-level PMUs.

Volatility

One potential means of establishing the amount of PV generation on a network is through the use of voltage volatility measurements. Volatility, an expression of the extent to which the voltage at a measurement point makes sudden, sharp changes in time, can serve as an indicator of nearby PV presence. The output of a solar panel is usually more dramatically dependent on external conditions than is the output of a legacy generator; passing clouds and unexpected shading are enough to cause large reductions in PV output. Over the course of a day, then, we would expect to see more voltage swings near PV panels than at similarly-loaded sites without PV.

Researchers have a great deal of flexibility in defining a metric for voltage volatility. To begin, our team has decided to use a simple measure: the absolute difference between the present (time t_0) voltage magnitude and the voltage magnitude at the past time $t_0 - X$.

$$volatility(t) = abs(V_{mag}(t) - V_{mag}(t - X)) \tag{1}$$

Examining the statistics of that measure over set periods of time of length N gives us some idea of the way that voltage volatility changes between N-sized time intervals.

We relied on previous research to select an appropriate X value across which to compare

voltage magnitudes. In particular, the LBNL report "Dark Shadows"[1] was very helpful. The researchers involved described correlations between 1-minute differences in PV output and external events such as passing clouds. On the strength of that work, we elected to use X values in the range of 1 minute as the most appropriate for our PV-discovery purposes. We selected an N-interval value of 1 hour based on the availability of historical hourly weather and irradiance conditions from Weather Underground.[2]

We are in the process of analyzing this data and have already seen some interesting characteristics appear in graphs of daily volatility. With an initial X value of 10 seconds, the volatility appears to roughly track the movement of the sun at a μPMU measuring a point that we believe to be a PV generator. Though it is far too early to draw any definite conclusions, if this tracking proves to be a dependable phenomenon on further testing, volatility analysis may lead to robust μPMU-based capabilities in PV discovery.

[1]Mills, A., Ahlstrom, M., Brower, M., Ellis, et. al. (2011). Dark Shadows. *IEEE Power and Energy Magazine, 9*(3), 33-41. doi:10.1109/mpe.2011.940575

[2]https://www.wunderground.com/